Original Article

JCBFM

Journal of Cerebral Blood Flow & Metabolism
2021, Vol. 41(9) 2344–2355

DOI: 10.1177/0271678X21996176
journals.sagepub.com/home/jcbfm
SAGE

Brain energy metabolism in intracerebroventricularly administered streptozotocin mouse model of Alzheimer's disease: A ^{1}H-[^{13}C]-NMR study

Narayan D Soni[1], Akila Ramesh[1,2], Dipak Roy[1] and Anant B Patel[1,2]

Abstract

Alzheimer's disease (AD) is a very common neurodegenerative disorder. Although a majority of the AD cases are sporadic, most of the studies are conducted using transgenic models. Intracerebroventricular (ICV) administered streptozotocin (STZ) animals have been used to explore mechanisms in sporadic AD. In this study, we have investigated memory and neurometabolism of ICV-STZ-administered C57BL6/J mice. The neuronal and astroglial metabolic activity was measured in ^{1}H-[^{13}C]-NMR spectrum of cortical and hippocampal tissue extracts of mice infused with [1,6-$^{13}C_2$] glucose and [2-^{13}C]acetate, respectively. STZ-administered mice exhibited reduced ($p = 0.00002$) recognition index for memory. The levels of creatine, GABA, glutamate and NAA were reduced ($p \leq 0.04$), while that of *myo*-inositol was increased ($p < 0.05$) in STZ-treated mice. There was a significant ($p \leq 0.014$) reduction in aspartate-C3, glutamate-C4/C3, GABA-C2 and glutamine-C4 labeling from [1,6-$^{13}C_2$]glucose. This resulted in decreased rate of glucose oxidation in the cerebral cortex (0.64 ± 0.05 *vs.* 0.77 ± 0.05 μmol/g/min, $p = 0.0008$) and hippocampus (0.60 ± 0.04 *vs.* 0.73 ± 0.07 μmol/g/min, $p = 0.001$) of STZ-treated mice, due to similar reductions of glucose oxidation in glutamatergic and GABAergic neurons. Additionally, reduced glutamine-C4 labeling points towards compromised synaptic neurotransmission in STZ-treated mice. These data suggest that the ICV-STZ model exhibits neurometabolic deficits typically observed in AD, and its utility in understanding the mechanism of sporadic AD.

Keywords

Cerebral metabolic rate, GABA, glutamate, glutamine, neurotransmission

Received 4 September 2020; Revised 29 January 2021; Accepted 29 January 2021

Introduction

Alzheimer's disease (AD) is the most common neurodegenerative disorder, and a leading cause of dementia worldwide. It is characterized by a progressive loss of memory, compromised intellectual abilities and cognitive functions.[1] According to the popular *amyloid cascade hypothesis*, genetic or environmental factors are considered as the primary cause of AD. These factors induce amyloid-beta (Aβ) aggregation and tau hyper-phosphorylation followed by the formation of toxic Aβ oligomers, plaques and neurofibrillary tangles (NFTs), ultimately leading to neurodegeneration and dementia.[2]

AD has been broadly categorized into familial and sporadic (sAD)[3] based on the genetic and non-genetic cause of its origin. Although sAD accounts for a majority of patients (95%),[4] the underlying mechanism in its onset and progression is least explored. Hence, there is a need for detailed investigations of different aspects of pathophysiology and mechanism of sAD using non-transgenic models.[5] Several chemical

[1]NMR Microimaging and Spectroscopy, CSIR-Centre for Cellular and Molecular Biology, Hyderabad, India
[2]Academy of Scientific and Innovative Research, Ghaziabad, India

Corresponding author:
Anant B Patel, NMR Microimaging and Spectroscopy, Centre for Cellular and Molecular Biology, Uppal Road, Habsiguda, Hyderabad 500 007, India.
Email: abpatel@ccmb.res.in

interventions have been used in rats and mice to develop sAD models.[6] These include administration of Aβ peptides, scopolamine, streptozotocin (STZ), L-methionine and heavy metals. Intracerebroventricular (ICV) STZ administration is widely used to model sAD in rodents.[7] It induces an insulin-resistant brain state[8] that arises due to impaired insulin response signaling,[9] ultimately leading to decreased glucose transport and metabolism, overproduction of Aβ peptides, tau hyperphosphorylation and neurofilaments in the brain.[8–11] The reduction in cerebral glucose metabolism has been considered as a key event in inducing AD-like phenotypes in ICV-STZ-treated animals. These features strengthen the relevance of the ICV-STZ model in understanding the pathophysiology of sporadic AD.

Glutamate and γ-aminobutyric acid (GABA) are the major excitatory and inhibitory neurotransmitters, respectively, in the matured mammalian central nervous system.[12] These neurotransmitters play major roles in cortical excitability and cognitive functions including learning and memory. The rates of neurotransmitter cycling and cerebral metabolic rates (CMR) of glucose oxidation in glutamatergic and GABAergic neurons have been shown to be reduced in transgenic[13–15] and chemical[16] models of AD. In contrast, the rate of acetate oxidation, a marker of astroglial metabolic activity, has been reported to be increased in AβPP-PS1 mice at the stage of high plaque load.[13]

Although cerebral glucose hypometabolism is proposed to be the initial event in the entire cascade of AD pathology, there is a limited quantitative measurement of neuronal and astroglial metabolic activity in STZ-treated mice. In this study, we have used ^{1}H-[^{13}C]-NMR spectroscopy in conjunction with infusion of [1,6-$^{13}C_2$]glucose and [2-^{13}C]acetate to quantitatively evaluate the neuronal and astroglial metabolic activity, respectively, in ICV-STZ-treated mice. Our findings revealed a significant reduction in the rates of neuronal glucose oxidation and neurotransmitter cycling in the cerebral cortex and hippocampus of STZ-treated mice.

Materials and methods

Animal preparation

All experimental procedures with animals were approved by the Institutional Animal Ethics Committee of CSIR-CCMB, and conducted in accordance with the guidelines established by the Committee for the Purpose of Control and Supervision of Experiments on Animals, Ministry of Environment and Forests, Government of India. ARRIVE guidelines were followed for the preparation of the manuscript. C57BL6/J mice were procured from the Jackson Laboratory (New Harbor, Maine, USA), bred and maintained in the CCMB Animal House Facility. Mice were housed in individually ventilated cages, and maintained at standard room temperature ($25 \pm 2^{\circ}$C) in a 12/12 h light and dark cycle with *ad libitum* access to food and water. Six-month-old male mice weighing 28 to 30 g were used for the study. Two sets of experiments were performed to understand the dose dependence of STZ (3 and 5 mg/kg). In a pilot study involving lower dose (3 mg/kg), a total of 16 mice were randomly assigned into two groups: ICV-STZ (n = 8) and Control (vehicle-injected) (n = 8). For the final experiment that involved STZ dose 5 mg/kg, mice were allocated equally to the ICV-STZ (n = 18) and control (n = 18) group. Investigators were familiar with the animals allocated to ICV-STZ and control groups, and there was no blinding used during the study.

Intracerebroventricular injection of streptozotocin

Mice were anesthetized using a combination of ketamine:xylazine (100:7.5 mg/kg, intraperitoneal), and positioned on a stereotaxic apparatus (Stoelting Co., USA). Two holes were drilled in the cranium (1.7 mm lateral, 0.3 mm posterior and 2.6 mm ventral from the bregma with an angle of 16° lateral from the dorso-ventral axis) for bilateral administration of STZ.[17] A fresh solution of STZ was prepared in artificial cerebrospinal fluids (aCSF, 20 mmol/L citrate buffer, pH 4.2) for the individual mouse to provide the required dose in 2 µl. STZ (1 µL) was administered into each lateral ventricle using a 5 µL micro-syringe mounted with a 32-gauge needle (Hamilton, USA) in 150 s. Control mice received the same volume of vehicle (aCSF in citrate buffer). One animal from each group died in the experiment with the lower dose of STZ (3 mg/kg), whereas three animals from each group died at the higher dose (5 mg/kg) during the entire study period (Figure 1(a)).

Memory assessment

The memory of mice was assessed two months post-STZ treatment using the Novel Object Recognition Test (NORT).[18] In brief, mice were initially trained to explore two identical objects placed at two corners in a rectangular wooden box ($35\times45\times30$ cm^3) for a period of 5 min. One-hour post-training, each mouse was further reintroduced into the box, wherein one of the familiar objects was replaced with a novel one, and the mouse was allowed to explore the objects again for 5 min. The recognition index (RI) of mice for the novel object was obtained as follows:

$$RI = \left(\frac{t_N}{t_F + t_N}\right) \times 100 \quad (1)$$

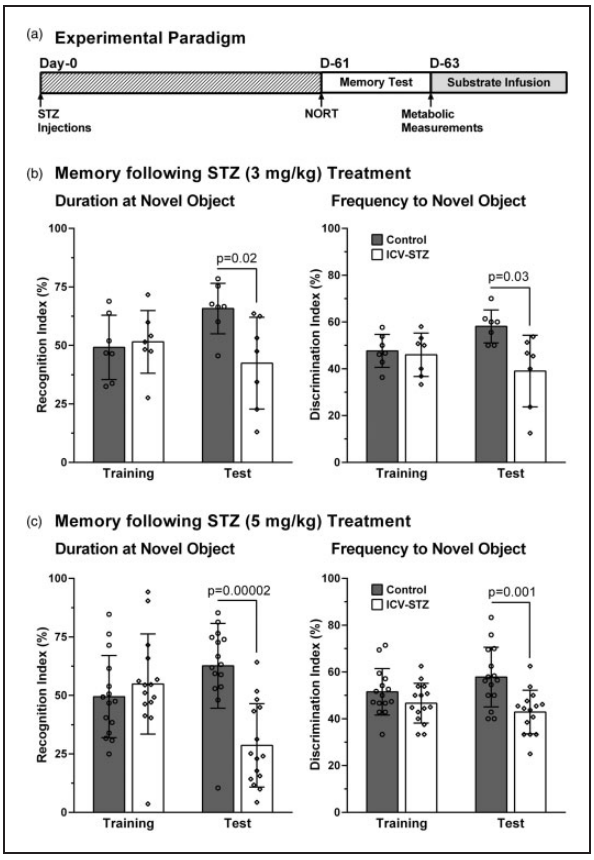

Figure 1. (a) Schematic representation of experimental paradigm. STZ was administered on the 0th day. The memory assessment was carried out on the 61st day, and the neurometabolic analysis on the 63rd day following infusion of [1,6-$^{13}C_2$]-glucose/[2-^{13}C]-acetate. Memory of the mice after (b) ICV-STZ (3 mg/kg), (c) ICV-STZ (5 mg/kg) treatment. The left and right panels depict the recognition and discrimination indices, respectively. Mice were first trained with two identical objects for 5 min. The working memory of mice was evaluated 1 h after the training by replacing the first object with a novel one. The recognition and discrimination indices were calculated using equations (1) and (2), respectively. The bar represent the mean± SD of the groups, while symbols denote individual values.

where t_F and t_N are the time spent by animals around the familiar and novel objects, respectively.

The ability of the animal to discriminate between objects was assessed using the frequency of visits to the novel object. The discrimination index (DI) for novel object was calculated as follows:

$$DI = \left(\frac{f_N}{f_F + f_N}\right) \times 100 \qquad (2)$$

where f_F and f_N are the frequency of visits by the animal to the familiar and novel objects, respectively.

Infusion of [1,6-$^{13}C_2$]glucose and [2-^{13}C]acetate

Mice were fasted for 4 h before metabolic measurement. The lateral tail vein was catheterized for the infusion of ^{13}C-labeled substrates.[19] In brief, [1,6-$^{13}C_2$]glucose (Cambridge Isotope Laboratories, Andover, MA, USA) dissolved in water (0.225 mol/L) was administered with an initial bolus rate of 1575 µmol/kg/min for the first 20 s. The infusion rate was stepped down exponentially at every 20 s to attain the final rate of 247 µmol/kg/min at 100 s, and was continued till 120 s. For assessment of astroglial metabolic activity, a solution of sodium [2-^{13}C]acetate (1 mol/L, Cambridge Isotope Laboratories, Andover, MA, USA) and D-glucose (0.225 mol/L, Sigma-Aldrich Inc., St. Louis, MO, USA) was prepared, and pH adjusted to 7.0. The sodium [2-^{13}C]acetate solution was delivered in mice using an infusion protocol.[20] A bolus of [2-^{13}C]acetate was administered with an initial rate of 10 mmol/kg/min during the first 15 s, and the rate was stepped down exponentially in four steps to 0.50 mmol/kg/min by 75 s, which continued till 120 s. Mice were released to home cage immediately after completion of the substrate infusion. The brain metabolism in mice infused with [1,6-$^{13}C_2$]glucose and [2-^{13}C]acetate was arrested using Focused Beam Microwave Irradiation system (4 kW, 1 s), (MMW-05, Muromachi Kikai Co., Ltd. Japan)[21] at 7 and 10 min, respectively.

Extraction of metabolites

The cerebral cortex and hippocampus were dissected from Microwave fixed brain. Tissue was weighed and homogenized with 0.1 N HCl in methanol (2:1 vol/wt) using a battery-operated tissue homogenizer (Argos Technologies, France) in a wet-ice bath.[22] [2-^{13}C]Glycine (100 µl, 2 mmol/L, Cambridge Isotope Laboratories, Andover, MA, USA) was added as an internal concentration reference. The mixture was homogenized in 60% ethanol (6:1 vol/wt). The homogenate was centrifuged at 15000 g for 45 min, and the supernatant was lyophilized. The freeze-dried powder was dissolved in 550 µl D_2O containing 0.25 mmol/L sodium 3-(trimethylsilyl)-2,2′,3,3′-D_4-propionate (TSP) for NMR analysis.

Acetate, being a volatile molecule, is lost during lyophilization in the routine extraction procedure. Hence, ^{13}C labeling of brain [2-^{13}C]acetate was measured in the brain stem extract. In brief, the brain stem was homogenized in 550 µl D_2O containing 1 mmol/L sodium formate. The homogenate was centrifuged, and the supernatant was used for NMR analysis.

^{1}H-[^{13}C]-NMR spectroscopy of brain tissue extracts

The NMR spectra of brain tissue extracts were recorded using a 600 MHz NMR spectrometer (Bruker Biospin, Ettlingen, Germany). The ^{1}H NMR spectra of brain stem extracts were obtained using pulse acquired sequence. The concentrations of metabolites in the cerebral cortex and hippocampus were measured in ^{1}H-[^{13}C]-NMR spectra of brain tissue extracts.[23,24] The levels of cerebral metabolites were calculated from the area of the respective peaks in the unedited spectrum relative to [2-^{13}C]glycine (added during metabolites extraction) measured in the ^{13}C edited spectrum. The percent ^{13}C enrichment of metabolites at various carbon positions was determined from the ratio of the area in the difference spectrum to the non-edited. The ^{13}C enrichments were reported after subtracting the natural abundance (1.1%) of carbon-13.

Estimation of astroglial and neuronal flux

The astroglial metabolic activity was investigated by monitoring the labeling of brain amino acids from [2-^{13}C]acetate, which is selectively transported into astroglia.[25] Acetate metabolism through the astroglial TCA cycle transfers ^{13}C label into the astroglial (small compartment) glutamate-C4 (Glu_{C4}) pool,[26] which is subsequently converted to glutamine-C4 (Gln_{C4})[20,27] by glutamine synthetase (glutamate ammonia ligase), an enzyme exclusively localized in the astrocytes.[28] The labeling of Glu_{C4} and GABA-C2 ($GABA_{C2}$) occurs through glutamate-glutamine and GABA-glutamine cycling, respectively. Aspartate-C2/C3 ($Asp_{C2/C3}$), $GABA_{C3/C4}$ and $Glu_{C2/C3}$ are labeled due to further metabolism of $GABA_{C2}$ and Glu_{C4} in the respective TCA cycle. The kinetics of ^{13}C labeling of amino acids from [2-^{13}C]acetate is shown to be linear till 30 min in the rat cerebral cortex.[20,29] The cerebral metabolic rate of acetate oxidation ($CMR_{Ace(Ox)}$) was calculated based on the ^{13}C label trapped into different amino acids from [2-^{13}C]acetate in 10 min using the following expression:[13]

$$CMR_{Ace(Ox)} = \frac{1}{10} \times \frac{1}{f_{Ace}} \times \left\{ \begin{array}{l} Glu_{C4} + GABA_{C2} + Gln_{C4} \\ \quad + 2\ (Asp_{C3} + Glu_{C3} + GABA_{C4}) \end{array} \right\} \quad (3)$$

where f_{Ace} is the fractional enrichment of [2-^{13}C]acetate, and Asp_{Ci}, $GABA_{Ci}$, Gln_{Ci} and Glu_{Ci} are the concentrations of ^{13}C labeled amino acids at 'i^{th}' carbon from [2-^{13}C]acetate.

The oxidation of [1,6-$^{13}C_2$]glucose in the glutamatergic and GABAergic neurons through the TCA cycle labels α-ketoglutarate-C4, which undergoes transamination to label Glu_{C4}.[13,19] In GABAergic neurons, Glu_{C4} is decarboxylated to $GABA_{C2}$ by glutamate decarboxylase. Astrocytic Gln_{C4} is labeled *via* cycling of Glu_{C4} and $GABA_{C2}$ followed by the action of glutamine synthetase. Further metabolism of glutamate and GABA in the TCA cycles labels $Asp_{C2/C3}$, $Glu_{C2/C3}$, $GABA_{C3/C4}$ and $Gln_{C2/C3}$. The labeling of amino acids has been shown to be linear till 20 min of glucose infusion in rats[30,31], mice[19] and human brain[32]. The rate of glucose oxidation in glutamatergic neurons ($CMR_{Glc(Glu)}$) was estimated from label trapped into amino acids from [1,6-$^{13}C_2$]glucose as described previously.[31,33]

$$CMR_{Glc(Glu)} = \frac{1}{7} \times \frac{1}{f_{Glc}} \times \left\{ \begin{array}{r} fGlu_{Glu}(Glu_{C4} + 2Glu_{C3}) \\ + fAsp_{Glu}(2Asp_{C3}) \end{array} \right\} \quad (4)$$

where f_{Glc} is the fractional enrichment of [1,6-$^{13}C_2$]glucose, while Asp_{Ci} and Glu_{Ci} are the levels of ^{13}C labeled amino acids at 'i^{th}' carbon in 7 min. $fAsp_{(Glu)}$ and $fGlu_{(Glu)}$ are the fractions of aspartate and glutamate in glutamatergic neurons as described previously.[19]

The rate of glucose oxidation in GABAergic neurons ($CMR_{Glc(GABA)}$) was determined as follows:

$$CMR_{Glc(GABA)} = \frac{1}{7} \times \frac{1}{f_{Glc}} \times \left\{ \begin{array}{r} fGlu_{GABA}(Glu_{C4} + 2Glu_{C3}) + (GABA_{C2} \\ + 2GABA_{C4}) + fAsp_{GABA}(2Asp_{C3}) \end{array} \right\} \quad (5)$$

where $GABA_{Ci}$ represents the concentration of labeled GABA at 'i^{th}' carbon from [1,6-$^{13}C_2$]glucose; $fAsp_{(GABA)}$ and $fGlu_{(GABA)}$ represent the fraction of aspartate and glutamate present in GABAergic neurons as described earlier.[19]

The total rate of glucose oxidation including neurons and astrocytes was estimated as follows:

$$CMR_{Glc(Total)} = \frac{1}{7} \times \frac{1}{f_{Glc}} \times \{Glu_{C4} + GABA_{C2} + Gln_{C4} + 2(Asp_{C3} + Glu_{C3} + GABA_{C4}) \quad (6)$$

where Gln_{C4} represents the concentration of ^{13}C labeled trapped into glutamine-C4 from [1,6-$^{13}C_2$]glucose in 7 min.

Estimation of rate of ATP synthesis

The rate of ATP synthesis was estimated by accounting for all the energy-rich molecules such as NADH, $FADH_2$ including ATP/GTP that are produced during the metabolism of glucose via glycolysis and

TCA cycle. The rates of glucose oxidation in glutamatergic and GABAergic neurons derived using equations (4) and (5) were used as primary flux together with a stoichiometry of 32 ATP for each glucose molecule.

Statistics

Unless stated, the data presented in the results correspond to the 5 mg/kg dose of STZ. All the statistical analyses were carried out using GraphPad Prism software (Ver 6.01, San Diego, USA). The Kolmogorov-Smirnov test was performed to assess the distribution of each data set. The significance of the difference of various measurements in ICV-STZ-treated and control mice was determined from the 2-tailed Student's T-test with Welch's correction. For a few data sets that did not pass the normality, the significance of difference was obtained using the Mann-Whitney U test. The data resulting in a p-value less than 0.05 were considered different from each other.

Results

Memory of ICV-STZ-treated mice

The memory of mice was assessed 60 days post STZ treatment using NORT. There was no significant difference ($p \geq 0.46$) in recognition index (RI) and discrimination index (DI) of STZ-treated mice (3 and 5 mg/kg) during training when compared to controls (Figure 1(b) and (c)). However, during the test phase, when one of the objects was replaced with a novel object, RI and DI of STZ-treated mice decreased significantly ($p \leq 0.03$) when compared with controls (Figure 1(b) and (c)).

Neurometabolites homeostasis in STZ-treated mice

The levels of neurometabolites were measured in the non-edited ^{1}H-[^{13}C]-NMR spectra from cortical and hippocampal tissue extracts (Figures 2 and 1S). There was a minor though significant ($p \leq 0.02$) reduction in NAA, taurine and creatine levels in the cerebral cortex and hippocampus of mice treated with the lower dose of STZ (3 mg/kg) (Table 1S). Additionally, there was a reduction ($p = 0.04$) in the cortical glutamate with STZ-treatment. The changes in brain metabolite homeostasis were more pronounced at the higher dose of STZ (5 mg/kg). This includes a reduction in glutamate (STZ 11.6 ± 0.8 μmol/g, $n = 15$; Control 12.4 ± 0.6 μmol/g, $n = 15$, $p = 0.005$), GABA (2.2 ± 0.1 *vs.* 2.3 ± 0.2 μmol/g, $p = 0.01$), NAA (6.0 ± 0.4 *vs.* 6.5 ± 0.4 μmol/g, $p = 0.001$) and creatine (12.1 ± 0.9 *vs.* 13.1 ± 1.2 μmol/g, $p = 0.02$) levels in the cerebral cortex (Table 1). Likewise, levels of glutamate (STZ 10.8 ± 0.6 μmol/g, $n = 15$; Control 11.6 ± 0.7 μmol/g, $n = 15$, $p = 0.002$), GABA (2.7 ± 0.1 *vs.* 3.0 ± 0.4 μmol/g, $p = 0.005$), NAA (6.0 ± 0.3 *vs.* 6.6 ± 0.5 μmol/g, $p = 0.002$), taurine (7.8 ± 0.6 *vs.* 8.6 ± 1.2 μmol/g, $p = 0.03$) and creatine (12.7 ± 0.5 *vs.* 13.5 ± 0.9 μmol/g, $p = 0.002$) were decreased in the hippocampus of mice treated with STZ. In contrast, the level of *myo*-Inositol was increased in the cerebral cortex ($p = 0.04$) and hippocampus ($p = 0.02$) of STZ-treated mice (Table 1).

Astroglial metabolic activity in STZ-treated mice

Representative ^{1}H-[^{13}C]-NMR spectra of cortical tissue extract of mice infused with [2-^{13}C]acetate are presented in Figure 1S. Prominent signals of Gln_{C4} (2.46 ppm) and Glu_{C4} (2.34 ppm) could be seen in the ^{13}C edited spectrum (lower panel) in the control and STZ-treated mice (5 mg/kg) (Figure 1S). Additionally, labeling of Asp_{C3}, $GABA_{C2}$ and Glu_{C3} could be seen. There was no significant difference in the ^{13}C labeling of cortical ($p \geq 0.14$) and hippocampal ($p \geq 0.45$) amino acids in STZ-treated mice when compared with respective controls (Table 2S). Consequently, the cerebral metabolic rate of acetate oxidation ($CMR_{Ace(Ox)}$) was unperturbed in the cerebral cortex (STZ 0.139 ± 0.010 μmol/g/min, $n = 8$; Control 0.142 ± 0.008 μmol/g/min, $n = 8$, $p = 0.55$) and hippocampus (0.152 ± 0.010 *vs.* 0.151 ± 0.012 μmol/g/min, $p = 0.89$) of STZ-treated mice. (Table 2S).

Metabolism of [1,6-$^{13}C_2$]glucose in STZ-treated mice

^{1}H-[^{13}C]-NMR spectra showing the labeling of cortical amino acids from [1,6-$^{13}C_2$]glucose in ICV-STZ-treated (5 mg/kg) mice and controls are presented in Figure 2. Labeling of different metabolites could be seen in the ^{13}C edited spectrum (lower panel) from control and ICV-STZ-treated mice (Figure 2(a) and (b)). Mice treated with the lower dose of STZ (3 mg/kg) exhibited a small but significant reduction in the labeling of Glu_{C4} ($P < 0.05$) and $GABA_{C2}$ ($P < 0.01$) from [1,6-$^{13}C_2$]glucose in the cerebral cortex and hippocampus (Table 3S). Moreover, the concentration of Glu_{C3} and Gln_{C4} was decreased in the cerebral cortex. Treatment with higher dose of STZ (5 mg/kg) leads to a reduction in the labeling of Asp_{C3} (STZ 0.27 ± 0.03 μmol/g, $n = 7$; Control 0.32 ± 0.03 μmol/g, $n = 7$, $p = 0.007$) together with $GABA_{C2}$ (0.29 ± 0.03 *vs.* 0.34 ± 0.02 μmol/g, $p = 0.001$), Gln_{C4} (0.37 ± 0.02 *vs.* 0.43 ± 0.04 μmol/g, $p = 0.004$) and Glu_{C3} (0.49 ± 0.06 *vs.* 0.60 ± 0.04 μmol/g, $p = 0.005$) and Glu_{C4} (2.16 ± 0.24 *vs.* 2.59 ± 0.22 μmol/g, $p = 0.005$) in the cerebral cortex (Figure 2, Table 2). The hippocampus exhibited profound reduction ($P \leq 0.009$) in the labeling of these amino acids in the STZ-treated (5 mg/kg) mice

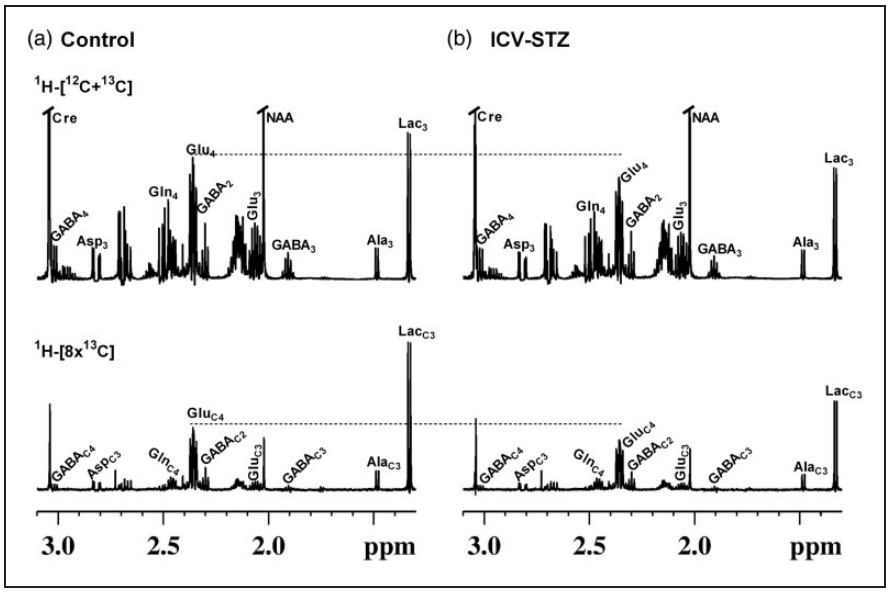

Figure 2. Representative ^{1}H-[^{13}C]-NMR spectra of cortical extracts from (a) Control, and (b) ICV-STZ (5 mg/kg) treated mice. Mice were infused with [1,6-$^{13}C_2$]glucose, and the brain metabolism was arrested using a focused beam microwave irradiation system immediately at 7 min of the infusion. Cortical metabolites were extracted using ethanol extraction protocol, and the NMR spectra were recorded using 600 MHz NMR spectrometer. Abbreviation used are: Ala_{C3}, alanine-C3; Asp_{C3}, aspartate-C3; Cre, creatine; $GABA_{C2}$, γ-aminobutyric acid-C2; $GABA_{C3}$, γ-aminobutyric acid-C3; $GABA_{C4}$, γ-aminobutyric acid-C4; Glu_{C3}, glutamate-C3; Glu_{C4}, glutamate-C4; Gln_{C4}, glutamine-C4; Lac_{C3}, Lactate-C3; NAA, N-acetyl aspartate.

Table 1. Concentration (μmol/g) of brain metabolites in STZ-treated (5 mg/kg) mice.

Brain regions	Treatment groups	Glu	GABA	Gln	Asp	NAA	m-Ino	Tau	Cho	p-Cho	GPC	Cre
Cerebral cortex	Control	12.4 ± 0.6	2.3 ± 0.2	4.5 ± 0.3	2.8 ± 0.2	6.5 ± 0.4	6.3 ± 0.4	10.2 ± 1.4	0.04 ± 0.01	0.78 ± 0.06	1.4 ± 0.1	13.0 ± 1.2
	ICV-STZ	11.6 ± 0.8**	2.2 ± 0.1*	4.5 ± 0.3	2.7 ± 0.3	6.0 ± 0.4**	6.7 ± 0.6*	9.5 ± 1.0	0.05 ± 0.01	0.77 ± 0.07	1.3 ± 0.1	12.1 ± 0.9*
Hippo-campus	Control	11.6 ± 0.7	3.0 ± 0.4	4.6 ± 0.3	2.5 ± 0.2	6.6 ± 0.5	6.9 ± 0.6	8.6 ± 1.2	0.05 ± 0.01	0.78 ± 0.06	1.3 ± 0.1	13.5 ± 0.9
	ICV-STZ	10.8 ± 0.6**	2.7 ± 0.1*	4.6 ± 0.3	2.4 ± 0.2	6.0 ± 0.3**	7.4 ± 0.5*	7.8 ± 0.6*	0.04 ± 0.01	0.75 ± 0.04	1.3 ± 0.1	12.7 ± 0.5**

The concentrations of metabolites were measured in the cortical and hippocampal tissue extracts from unedited ^{1}H-[^{13}C]-NMR spectrum using [2-^{13}C]glycine as reference. Values are presented as mean±SD. *$p < 0.05$ and **$p < 0.01$ when ICV-STZ-treated mice were compared with controls. Asp: aspartate; Cho: Choline; p-Cho: phosphocholine; GPC: glycerophosphocholine; Cre: creatine; GABA: γ-aminobutyric acid; Glu: glutamate; Gln: glutamine; ICV-STZ: intracerebroventricular-streptozotocin: m-Ino: myo-inositol; NAA: N-acetyl aspartate; Tau: Taurine.

(Table 2). The reduction in ^{13}C labeled Asp_{C3}, $Glu_{C4/C3}$, and $GABA_{C2}$ is suggestive of decreased cerebral glucose oxidation in the STZ-treated mice. Additionally, the reduced ^{13}C labeling of Gln_{C4} from [1,6-$^{13}C_2$]glucose suggests compromised neurotransmitter cycling in the cerebral cortex and hippocampus of STZ-treated mice.

Neurometabolic activity in STZ-treated mice

The rates of glucose oxidation in glutamatergic and GABAergic neurons were decreased ($p \leq 0.04$) slightly (~9%) following the lower dose of STZ-treatment (3 mg/kg) (Figure 3). The higher dose of STZ (5 mg/kg) resulted in further reduction in glucose oxidation in the cerebral cortex (STZ: 0.641 ± 0.050 μmol/g/min, n = 7; Control: 0.767 ± 0.053 μmol/g/min, n = 7, p = 0.0008) (Figure 4(a)). The decrease in the rate of glucose oxidation in the STZ-treated mice was contributed by a similar degree of reduction (~17%) in glutamatergic (0.401 ± 0.043 *vs.* 0.482 ± 0.033 μmol/g/min, p = 0.003) and GABAergic (0.103 ± 0.008 *vs.* 0.123 ± 0.013 μmol/g/min, p = 0.01) neuronal metabolic activity. Similarly, hippocampus exhibited a reduction (−18%) in glucose oxidation (0.599 ± 0.041 *vs.* 0.733 ± 0.068 μmol/g/min, p = 0.001) that was contributed by a decline in the rate of glucose oxidation in glutamatergic (0.370 ± 0.029 *vs.* 0.452 ± 0.042,

$p = 0.002$) and GABAergic neurons (0.119 ± 0.010 *vs.* 0.147 ± 0.015, $p = 0.003$) (Figure 4(c)).

ATP synthesis in STZ-treated mice

The rate of ATP synthesis was reduced significantly ($p = 0.0006$) in the cerebral cortex of ICV-STZ-treated (5 mg/kg) mice (20.5 ± 1.6 μmol/g/min) when compared with sham controls (24.6 ± 1.7 μmol/g/min). This reduction was due to a similar decline in ATP synthesis in glutamatergic (12.8 ± 1.4 *vs.* 15.4 ± 1.1 μmol/g/min, $p = 0.002$) and GABAergic neurons (3.3 ± 0.2 *vs.* 3.9 ± 0.4 μmol/g/min, $p = 0.006$) (Figure 4(b)). The hippocampus of STZ-treated mice also exhibited a similar reduction in the rate of ATP synthesis (19.2 ± 1.3 *vs.* 23.5 ± 2.2 μmol/g/min, $p = 0.001$) that was contributed by a decrease in the ATP production in glutamatergic (11.8 ± 0.9 *vs.* 14.5 ± 1.3 μmol/g/min, $p = 0.001$) and GABAergic (3.8 ± 0.3 *vs.* 4.7 ± 0.5 μmol/g/min, $p = 0.002$) neurons (Figure 4(d)).

Correlation between memory and neurometabolic activity

In order to understand the relation between memory and neurometabolic activity, a correlation analysis was carried out between the discrimination index (DI) and cerebral metabolic rate of glucose oxidation. A significant correlation was observed for cortical CMR_{Glc} ($R^2 = 0.42$; $p = 0.01$) and $CMR_{Glc(Glu)}$ ($R^2 = 0.44$; $p = 0.01$) with DI, whereas the correlation of $CMR_{Glc(GABA)}$ with DI was not very significant ($R^2 = 0.09$; $p = 0.20$) (Figure 5(a)). Likewise, the correlation of CMR_{Glc} ($R^2 = 0.46$; $p = 0.007$) and $CMR_{Glc(Glu)}$ ($R^2 = 0.48$; $p = 0.007$) with DI was significant in the hippocampus (Figure 5(b)). Additionally, $CMR_{Glc(GABA)}$ exhibited a fair relationship ($R^2 = 0.35$; $p = 0.02$) with DI. It is noteworthy that the correlation between neurometabolic and memory measures in the hippocampus ($R^2 = 0.35$ to 0.48) was reasonably better than that observed in the cerebral cortex ($R^2 = 0.09$ to 0.44).

Table 2. Concentration (μmol/g) of ^{13}C labeled amino acids from [1,6-$^{13}C_2$]glucose in STZ-treated (5 mg/kg) mice.

Brain regions	Treatment groups	Glu_{C4}	$GABA_{C2}$	Gln_{C4}	Asp_{C3}	Glu_{C3}	$GABA_{C4}$
Cerebral cortex	Control	2.59 ± 0.22	0.34 ± 0.02	0.43 ± 0.04	0.32 ± 0.03	0.60 ± 0.04	0.09 ± 0.03
	ICV-STZ	2.16 ± 0.24**	0.29 ± 0.03**	0.37 ± 0.02**	0.27 ± 0.03**	0.49 ± 0.06**	0.07 ± 0.03
Hippo-campus	Control	2.33 ± 0.27	0.38 ± 0.04	0.41 ± 0.04	0.40 ± 0.07	0.48 ± 0.05	0.12 ± 0.02
	ICV-STZ	1.92 ± 0.14**	0.30 ± 0.02**	0.35 ± 0.02**	0.31 ± 0.04**	0.39 ± 0.06**	0.10 ± 0.02

Mice were infused with [1,6-$^{13}C_2$]glucose for 2 min, and brain metabolism was arrested at 7 min using a focused beam microwave irradiation system. The concentrations of ^{13}C labeled amino acids at the specific carbon position were measured in tissue extracts in ^{13}C edited spectra using [2-^{13}C] glycine as reference. Values are presented as mean±SD. **$p < 0.01$ when ICV-STZ-treated mice were compared with controls.

Asp_{C3}: aspartate-C3; $GABA_{C2}$: γ-aminobutyric acid-C2; $GABA_{C4}$: γ-aminobutyric acid-C4; Glu_{C3}: glutamate-C3; Glu_{C4}: glutamate-C4; Gln_{C4}: glutamine-C4.

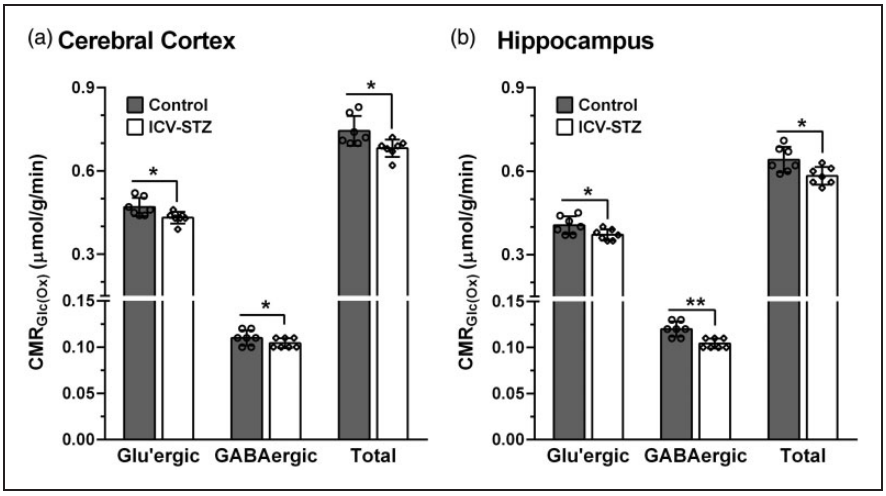

Figure 3. Cerebral Metabolic rates of glucose oxidation ($CMR_{Glc(Ox)}$) in (a) Cerebral cortex and (b) Hippocampus of ICV-STZ (3 mg/kg) treated mice. The ^{13}C labeling of amino acids from [1,6-$^{13}C_2$]glucose was measured in the tissue extracts using ^{1}H-[^{13}C]-NMR spectroscopy. The $CMR_{Glc(Ox)}$ was calculated using equations (4) to (6). The vertical bar represents the mean±SD of the group, while the symbols depict individual values. *$p < 0.05$ and **$p < 0.01$ when ICV-STZ-treated mice were compared with controls.

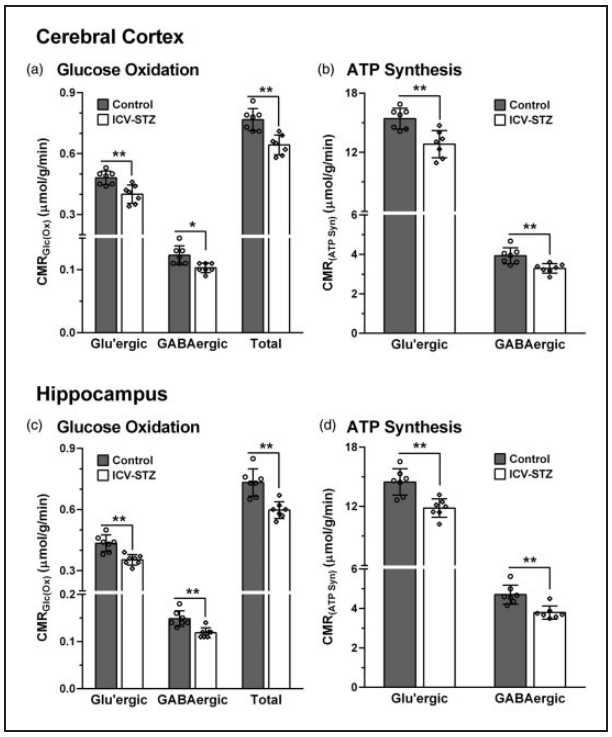

Figure 4. Cerebral Metabolic rates of: (a) Glucose oxidation ($CMR_{Glc(Ox)}$) and (b) ATP synthesis ($CMR_{ATP(Syn)}$) in the cerebral cortex of ICV-STZ-treated (5 mg/kg) mice; (c) $CMR_{Glc(Ox)}$, and (d) $CMR_{ATP(Syn)}$ in the hippocampus of STZ-treated mice. The ^{13}C labeling of amino acids from [1,6-$^{13}C_2$]glucose was measured in the tissue extracts using ^{1}H-[^{13}C]-NMR spectroscopy. The $CMR_{Glc(Ox)}$ was calculated using *Eqns.* (4) to (6). The ATP synthesis rate was determined by multiplying the CMR_{Glc} by a factor of 32. The vertical bar represents the mean±SD of the group, while the symbols depict individual values. *$p < 0.05$ and **$p < 0.01$ when ICV-STZ-treated mice were compared with controls.

Discussion

The very first case of AD was reported more than a century ago but the actual mechanism involved in its onset and progression is still not clear. Amyloid-β protein from AD brain was purified and characterized for the first time by Glenner and Wong in the early eighties.[34] This led to the identification of several mutations in APP, PS1 and PS2 proteins responsible for the formation of Aβ plaques. These findings supported the genetic basis of the disease in a subset of AD patients, and facilitated the generation of transgenic rodent models. However, these models could not provide the detailed mechanism of the disease. Hence, there is a pressing need for the use of alternate models for AD studies. ICV-STZ-administered mice and rats have been routinely used to explore the pathophysiology of sporadic AD. The current study was aimed at establishing the energetics involved in neuronal (glutamatergic and GABAergic) and astroglial metabolism in ICV-STZ-treated mice. Similar to previous reports, our results show impaired memory in STZ-treated animals.[35]

^{1}H NMR spectroscopy has been used extensively to assess the levels of several key brain metabolites in patients and animal models of AD. These studies suggested a reduction in the levels of cortical NAA,[36] GABA and glutamate,[15] while an increase in that of myo-inositol[37] in AD. Our findings of a reduction in levels of glutamate, GABA, creatine and NAA together with an increased *myo*-inositol in STZ-treated mice is in consistence with previous reports in transgenic AβPP-PS1 mouse,[13,14] $AlCl_3$-treated C57BL6/J mouse[16] and ICV-STZ-treated rat[38] models of AD. The concurrent reduction of glutamate and NAA levels in STZ-treated mice suggests reduced viability or population of glutamatergic neurons. Glutamate is known to be involved in the control of different cognitive functions including learning and memory through long-term potentiation. The reduction in glutamate level probably explains the poor memory of ICV-STZ-treated mice. The increased level of *myo*-inositol in STZ-treated mice suggests an increase in the population or activity of astroglial cells, possibly due to increased inflammatory response that exists in the AD brain.[39] Additionally, hypertonic extracellular condition increases inflow of myo-inositol into cells leading to an increase in its cellular content.[40]

Although the brain contributes only ~2% of total body weight, it utilizes ~20% of the total oxygen and glucose indicating the overwhelming energy demand of the brain. Such high energy is required to support the neuronal functions associated with action potentials, resting potentials, neurotransmitter release and recycling.[41] Decrease in the rate of glucose metabolism leads to reduced ATP production, and increased risk of oxidative damage, which have profound consequences on brain functioning.[42] The failure to fulfill the energy demand of the brain is known to increase the risk of Aβ formation and aggregation in APP_{SWE} mice.[43] In fact, glucose hypometabolism is one of the prominent and key characteristics of the AD brain. PET studies have indicated a widespread reduction in brain glucose consumption in the posterior cingulate, lateral temporoparietal and occipital cortices of AD patients.[44,45] Additionally, glucose hypo-metabolism has been observed in the temporoparietal and posterior cingulate brain regions of subjects with mild cognitive impairment.[46] Moreover, we have reported a reduction in brain glucose oxidation in 6-month-old AβPP-PS1 mice, which bears resemblance to the preclinical stage of AD.[14] There is very limited information about the status of cerebral glucose metabolism in ICV-STZ

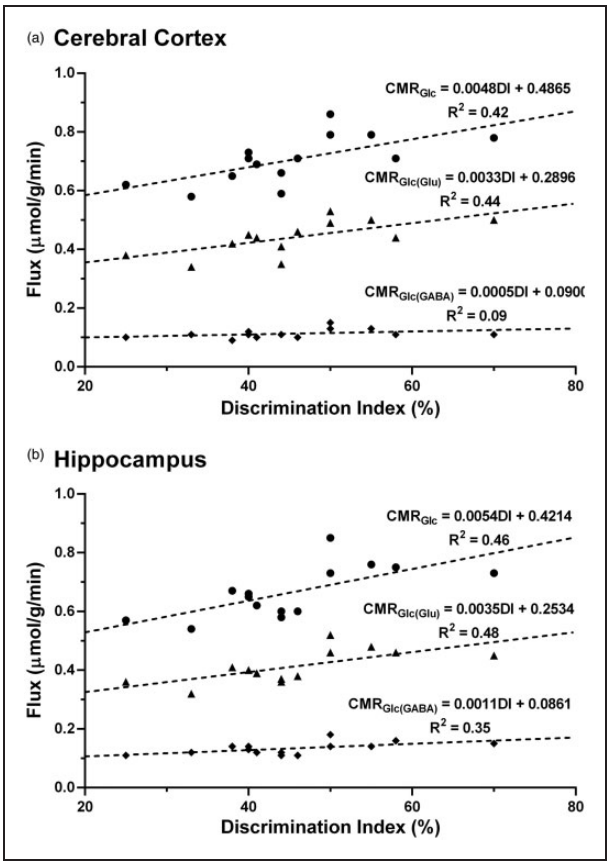

Figure 5. The correlation between memory and neurometabolic measures (● CMR_{Glc}, ▲ $CMR_{Glc(Glu)}$, ◆ $CMR_{Glc(GABA)}$) in (a) Cerebral cortex and (b) Hippocampus of control and ICV-STZ-treated (5 mg/kg) mice. Discrimination Index (DI) was calculated using equation (2), based on the frequency of animals towards novel object in the novel object recognition test. The cerebral rates of glucose oxidation were measured from the ^{13}C labeling of amino acids from [1,6-$^{13}C_2$]glucose using equations (4) to (6).

animals. A reduction in brain glucose utilization in the parietal cerebral cortex (−19%), frontal cerebral cortex (−13%) and different hippocampal regions (−12%) have been reported in the STZ-treated Wistar rats.[47] Consistent with this report, we observed a decrease in the rate of glucose oxidation in the cerebral cortex (−16%) and hippocampus (−18%).

Acetate metabolism has been used as a marker of astroglial metabolic activity and neuroinflammation. Analysis of neurometabolism in 12-month-old AβPP-PS1 mice revealed an increase in cerebral metabolic rate of acetate oxidation, indicating astrocyte-mediated neuroinflammation in AD.[13] Our attempts to understand the functional status of astroglia in STZ-treated mice revealed no change in the ^{13}C labeling of cortical and hippocampal amino acids from [2-^{13}C]acetate, suggesting that astroglial metabolic activity is unperturbed in these mice (Table 2S). Hence, the finding of increased myo-inositol level in STZ-treated mice suggests hypertonicity of extracellular fluids in cortical and hippocampal volume.[40]

This study sheds light on the functional status of excitatory and inhibitory neurons in ICV-STZ-treated mice. Our data indicated a reduction in the label incorporation in $Glu_{C4/C3}$ and $GABA_{C2/C4}$ from [1,6-$^{13}C_2$]glucose in the cerebral cortex and hippocampus of STZ-treated mice (Table 2). These findings suggest a reduction in the excitatory and inhibitory activity related to glutamatergic and GABAergic neurons, respectively (Figure 4(a) and (c)). The reduction of glucose oxidation in the cerebral cortex and hippocampus of STZ-treated mice was contributed by almost an identical reduction in the rates of glucose oxidation in excitatory (−17%) and inhibitory neurons (−18%). The neuronal glucose oxidation flux is shown to be stoichiometrically coupled with the rate of neurotransmitter cycling.[48,49] Hence, a reduction in the neuronal glucose oxidation in glutamatergic and GABAergic neurons in the ICV-STZ-treated mice suggests reduced synaptic transmission in these mice. In fact, the level of ^{13}C label trapped into Gln_{C4}, which is labeled *via* glutamate-glutamine and GABA-glutamine cycling, was reduced in the cerebral cortex (−14%) and hippocampus (−16%) of STZ-treated mice (Table 2) further corroborate the interpretation.

Our analysis of the association between memory and neurometabolic measures showed a fairly good correlation for different fluxes in both brain regions (Figure 5). The total as well as glutamatergic neurometabolic rates were in a fairly good association with the memory in the cerebral cortex and hippocampus. However, a significant correlation (R^2) of GABAergic flux with episodic memory could be observed only in the hippocampus. This further validates our findings, as glutamate is known to play a direct role in the process of learning and memory through long term potentiation. Additionally, the correlation of GABAergic neurometabolic activity with the memory in the hippocampus emphasizes its role as the primary brain region responsible for memory.

Glucose metabolism serves as the primary source of energy through the process of oxidative phosphorylation via electron transport chain (ETC) in mitochondria. The derived energy is utilized to power neurotransmission and other vital neuronal functions in the brain. The disruption of ETC not only reduces the yield of ATP, but also increases the burden of oxidative stress, which is known to be a contributing factor in the majority of neurodegenerative disorders including AD.[42] Our analysis indicated that the efficiency of ATP synthesis was reduced to ~82% in the

cerebrum of STZ-treated mice. The reduced availability of ATP may be driving the brains of STZ-treated mice to an AD-like condition.[43]

There are a few limitations with regard to the current study. Firstly, the estimation of the cerebral metabolic rates in the current study assumes complete trapping of labels into amino acids. Any loss of label due to glutamine efflux from the brain will violate the assumption, and will underestimate the metabolic rates to the extent of the efflux. However, glutamine efflux (PC flux) is reported to be very small relative to pyruvate dehydrogenase.[50] Secondly, the expression used for the estimation of glucose oxidation in glutamatergic and GABAergic neurons does not account for the flow of label into glutamine. However, the labeling of glutamine in the control and STZ-treated mice is very small. Lastly, a small amount of ^{13}C label may be lost as CO_2 by oxidation in subsequent turns of the TCA cycle. Hence, the metabolic flux associated with glutamatergic and GABAergic neurons is likely to be underestimated. However, it could be argued that such losses would occur in control and ICV-STZ-mice. Therefore, although the absolute rates may be slightly lower in both groups, the directional changes in flux should remain valid.

The current study examines the impact of ICV-STZ administration on behavioral and cerebral metabolic measures in the mouse. Most importantly, it deciphers the energetics of astroglia, excitatory glutamatergic and inhibitory GABAergic neurons under the sporadic AD-like condition. The findings of the study revealed a compromised state of excitatory as well as inhibitory neurons, and reduced synaptic transmission in the ICV-STZ-administered mice. These results provide experimental evidence for impairment of neurotransmitter metabolism in STZ-treated mice, a model of sporadic AD.

Funding

The author(s) disclosed receipt of the following financial support for the research, authorship, and/or publication of this article: The study was supported by funding from CSIR-CCMB (NCP/MLP0139).

Declaration of conflicting interests

The author(s) declared no potential conflicts of interest with respect to the research, authorship, and/or publication of this article.

Authors' contributions

NDS: Animal experiments, Data acquisition, Analysis and Interpretation of Results, Manuscript writing.
AR: Animal experiments, Manuscript writing.
DR: Animal experiments, Manuscript writing.
ABP: Experimental design, Reagents and analytic tools, Analysis and Interpretation of Results, Manuscript writing, Supervised and directed the overall project.
All authors have read and approved the final manuscript.

Supplemental material

Supplemental material for this article is available online.

ORCID iD

Anant B Patel https://orcid.org/0000-0002-9551-9395

Acknowledgements

The authors wish to thank Dr. Robin de Graff at Yale University for providing the POCE pulse sequence, and Dr. T Ramakrishna (ex CCMB Scientist) for critical editing of the manuscript. We acknowledge the efforts of Ms. B. Jyothi Lakshmi and Mr. N. Sai Ram of the Animal House for the maintenance of quality animals. We also thank the CCMB Animal House and Behavioral Facility for providing the facility for surgical procedures and behavioral experiments. All NMR experiments were carried out in the NMR Microimaging and Spectroscopy Facility, CSIR-CCMB, Hyderabad, India.

References

1. Scheltens P, Blennow K, Breteler MM, et al. Alzheimer's disease. *Lancet* 2016; 388: 505–517.
2. Gilbert BJ. The role of amyloid beta in the pathogenesis of Alzheimer's disease. *J Clin Pathol* 2013; 66: 362–366.
3. Correia SC, Santos RX, Santos MS, et al. Mitochondrial abnormalities in a streptozotocin-induced rat model of sporadic Alzheimer's disease. *Curr Alzheimer Res* 2013; 10: 406–419.
4. Liu PP, Xie Y, Meng XY, et al. History and progress of hypotheses and clinical trials for Alzheimer's disease. *Signal Transduct Target Ther* 2019; 4: 29.
5. Lecanu L and Papadopoulos V. Modeling Alzheimer's disease with non-transgenic rat models. *Alzheimers Res Ther* 2013; 5: 17.
6. Li X, Bao X and Wang R. Experimental models of Alzheimer's disease for deciphering the pathogenesis and therapeutic screening (review). *Int J Mol Med* 2016; 37: 271–283.
7. Nitsch R and Hoyer S. Local action of the diabetogenic drug, streptozotocin, on glucose and energy metabolism in rat brain cortex. *Neurosci Lett* 1991; 128: 199–202.
8. Salkovic-Petrisic M, Tribl F, Schmidt M, et al. Alzheimer-like changes in protein kinase B and glycogen synthase kinase-3 in rat frontal cortex and hippocampus after damage to the insulin signalling pathway. *J Neurochem* 2006; 96: 1005–1015.
9. Deng Y, Li B, Liu Y, et al. Dysregulation of insulin signaling, glucose transporters, O-GlcNAcylation, and phosphorylation of tau and neurofilaments in the brain: implication for Alzheimer's disease. *Am J Pathol* 2009; 175: 2089–2098.

10. Blennow K, de Leon MJ and Zetterberg H. Alzheimer's disease. *Lancet* 2006; 368: 387–403.
11. Grunblatt E, Salkovic-Petrisic M, Osmanovic J, et al. Brain insulin system dysfunction in streptozotocin intracerebroventricularly treated rats generates hyperphosphorylated tau protein. *J Neurochem* 2007; 101: 757–770.
12. Erecińska M and Silver IA. Metabolism and role of glutamate in mammalian brain. *Prog Neurobiol* 1990; 35: 245–296.
13. Patel AB, Tiwari V, Veeraiah P, et al. Increased astroglial activity and reduced neuronal function across brain in AβPP-PS1 mouse model of Alzheimer's disease. *J Cereb Blood Flow Metab* 2018; 38: 1213–1226.
14. Tiwari V and Patel AB. Impaired glutamatergic and GABAergic function at early age in AβPPswe-PS1dE9 mice: implications for Alzheimer's disease. *J Alzheimers Dis* 2012; 28: 765–769.
15. Nilsen LH, Witter MP and Sonnewald U. Neuronal and astrocytic metabolism in a transgenic rat model of Alzheimer's disease. *J Cereb Blood Flow Metab* 2014; 34: 906–914.
16. Saba K, Rajnala N, Veeraiah P, et al. Energetics of excitatory and inhibitory neurotransmission in aluminum chloride model of Alzheimer's disease: reversal of behavioral and metabolic deficits by rasa sindoor. *Front Mol Neurosci* 2017; 10: 323.
17. Chen Y, Liang Z, Blanchard J, et al. A non-transgenic mouse model (ICV-STZ mouse) of Alzheimer's disease: similarities to and differences from the transgenic model (3xTg-AD mouse). *Mol Neurobiol* 2013; 47: 711–725.
18. Bevins RA and Besheer J. Object recognition in rats and mice: a one-trial non-matching-to-sample learning task to study 'recognition memory'. *Nat Protoc* 2006; 1: 1306–1311.
19. Tiwari V, Ambadipudi S and Patel AB. Glutamatergic and GABAergic TCA cycle and neurotransmitter cycling fluxes in different regions of mouse brain. *J Cereb Blood Flow Metab* 2013; 33: 1523–1531.
20. Patel AB, de Graaf RA, Rothman DL, et al. Evaluation of cerebral acetate transport and metabolic rates in the rat brain *in vivo* using ^{1}H-[^{13}C]-NMR. *J Cereb Blood Flow Metab* 2010; 30: 1200–1213.
21. de Graaf RA, Chowdhury GM, Brown PB, et al. In situ 3D magnetic resonance metabolic imaging of microwave-irradiated rodent brain: a new tool for metabolomics research. *J Neurochem* 2009; 109: 494–501.
22. Patel AB, Rothman DL, Cline GW, et al. Glutamine is the major precursor for GABA synthesis in rat neocortex *in vivo* following acute GABA-transaminase inhibition. *Brain Res* 2001; 919: 207–220.
23. Bagga P, Chugani AN, Varadarajan KS, et al. *In vivo* NMR studies of regional cerebral energetics in MPTP model of Parkinson's disease: recovery of cerebral metabolism with acute levodopa treatment. *J Neurochem* 2013; 127: 365–377.
24. de Graaf RA, Brown PB, Mason GF, et al. Detection of [1,6-$^{13}C_2$]-glucose metabolism in rat brain by *in vivo* ^{1}H-[^{13}C]-NMR spectroscopy. *Magn Reson Med* 2003; 49: 37–46.
25. Waniewski RA and Martin DL. Preferential utilization of acetate by astrocytes is attributable to transport. *J Neurosci* 1998; 18: 5225–5233.
26. Berl S and Frigyesi TL. The turnover of glutamate, glutamine, aspartate and GABA labeled with [1-14C]acetate in caudate nucleus, thalamus and motor cortex (cat). *Brain Res* 1969; 12: 444–455.
27. Cerdan S, Kunnecke B and Seelig J. Cerebral metabolism of [1,2-$^{13}C_2$]acetate as detected by *in vivo* and in vitro ^{13}C NMR. *J Biol Chem* 1990; 265: 12916–12926.
28. Norenberg MD and Martinez-Hernandez A. Fine structural localization of glutamine synthetase in astrocytes of rat brain. *Brain Res* 1979; 161: 303–310.
29. Xin L, Mlynarik V, Lanz B, et al. 1H-[13C] NMR spectroscopy of the rat brain during infusion of [2-13C] acetate at 14.1 T. *Magn Reson Med* 2010; 64: 334–340.
30. de Graaf RA, Mason GF, Patel AB, et al. Regional glucose metabolism and glutamatergic neurotransmission in rat brain in vivo. *Proc Natl Acad Sci USA* 2004; 101: 12700–12705.
31. Patel AB, de Graaf RA, Mason GF, et al. The contribution of GABA to glutamate/glutamine cycling and energy metabolism in the rat cortex *in vivo*. *Proc Natl Acad Sci U S A* 2005; 102: 5588–5593.
32. Shen J, Petersen KF, Behar KL, et al. Determination of the rate of the glutamate/glutamine cycle in the human brain by in vivo 13C NMR. *Proc Natl Acad Sci USA* 1999; 96: 8235–8240.
33. Mishra PK, Kumar A, Behar KL, et al. Subanesthetic ketamine reverses neuronal and astroglial metabolic activity deficits in a social defeat model of depression. *J Neurochem* 2018; 146: 722–734.
34. Glenner GG and Wong CW. Alzheimer's disease: initial report of the purification and characterization of a novel cerebrovascular amyloid protein. *Biochem Biophys Res Commun* 1984; 120: 885–890.
35. Grieb P. Intracerebroventricular streptozotocin injections as a model of Alzheimer's disease: in search of a relevant mechanism. *Mol Neurobiol* 2016; 53: 1741–1752.
36. Cheng LL, Newell K, Mallory AE, et al. Quantification of neurons in Alzheimer and control brains with *ex vivo* high resolution magic angle spinning proton magnetic resonance spectroscopy and stereology. *Magn Reson Imaging* 2002; 20: 527–533.
37. Marjanska M, Curran GL, Wengenack TM, et al. Monitoring disease progression in transgenic mouse models of Alzheimer's disease with proton magnetic resonance spectroscopy. *Proc Natl Acad Sci USA* 2005; 102: 11906–11910.
38. Labak M, Foniok T, Kirk D, et al. Metabolic changes in rat brain following intracerebroventricular injections of streptozotocin: a model of sporadic Alzheimer's disease. *Acta Neurochir Suppl* 2010; 106: 177–181.
39. Fuster-Matanzo A, Llorens-Martin M, Hernandez F, et al. Role of neuroinflammation in adult neurogenesis and Alzheimer disease: therapeutic approaches. *Mediators Inflamm* 2013; 2013: 260925.

40. Burg MB and Ferraris JD. Intracellular organic osmolytes: function and regulation. *J Biol Chem* 2008; 283: 7309–7313.
41. Howarth C, Gleeson P and Attwell D. Updated energy budgets for neural computation in the neocortex and cerebellum. *J Cereb Blood Flow Metab* 2012; 32: 1222–1232.
42. Angelova PR and Abramov AY. Role of mitochondrial ROS in the brain: from physiology to neurodegeneration. *FEBS Lett* 2018; 592: 692–702.
43. Velliquette RA, O'Connor T and Vassar R. Energy inhibition elevates β-secretase levels and activity and is potentially amyloidogenic in AβPP transgenic mice: possible early events in Alzheimer's disease pathogenesis. *J Neurosci* 2005; 25: 10874–10883.
44. de Leon MJ, Ferris SH, George AE, et al. Positron emission tomographic studies of aging and Alzheimer disease. *AJNR Am J Neuroradiol* 1983; 4: 568–571.
45. Rabinovici GD, Furst AJ, Alkalay A, et al. Increased metabolic vulnerability in early-onset Alzheimer's disease is not related to amyloid burden. *Brain* 2010; 133: 512–528.
46. Drzezga A, Lautenschlager N, Siebner H, et al. Cerebral metabolic changes accompanying conversion of mild cognitive impairment into Alzheimer's disease: a PET follow-up study. *Eur J Nucl Med Mol Imaging* 2003; 30: 1104–1113.
47. Duelli R, Schrock H, Kuschinsky W, et al. Intracerebroventricular injection of streptozotocin induces discrete local changes in cerebral glucose utilization in rats. *Int J Dev Neurosci* 1994; 12: 737–743.
48. Patel AB, de Graaf RA, Mason GF, et al. Glutamatergic neurotransmission and neuronal glucose oxidation are coupled during intense neuronal activation. *J Cereb Blood Flow Metab* 2004; 24: 972–985.
49. Sibson NR, Dhankhar A, Mason GF, et al. Stoichiometric coupling of brain glucose metabolism and glutamatergic neuronal activity. *Proc Natl Acad Sci USA* 1998; 95: 316–321.
50. Sibson NR, Mason GF, Shen J, et al. In vivo (13)C NMR measurement of neurotransmitter glutamate cycling, anaplerosis and TCA cycle flux in rat brain during. *J Neurochem* 2001; 76: 975–989.